

Developing and Testing the EPED Pedestal Model

P.B. Snyder¹, M.N.A. Beurskens², R.J. Groebner¹, J.W. Hughes³, R. Maingi⁴, T.H. Osborne¹, J.R. Walk³, H.R. Wilson⁵, Alcator C-Mod and DIII-D Teams, and JET-EFDA Contributors*

¹General Atomics, PO Box 85608, San Diego, CA 92186-5608, USA

²EURATOM /CCFE Fusion Association, Culham Science Centre, Abingdon, OX14 3DB, UK

³Massachusetts Institute of Technology, PSFC, Cambridge, MA 02139, USA

⁴Oak Ridge National Laboratory, Oak Ridge, TN 37831, USA

⁵York Plasma Institute, Dept of Physics, U. of York, UK

The pressure at the top of the edge transport barrier (or “pedestal height”) strongly impacts global confinement and fusion performance, while large edge localized modes (ELMs) can significantly limit component lifetimes. The EPED model [1–3] predicts the H-mode pedestal height and width based upon two fundamental and calculable constraints: 1) onset of non-local peeling-balloonning (P-B) modes at low to intermediate mode number, 2) onset of nearly local kinetic ballooning modes (KBM) at high mode number. The model calculates both constraints directly with no fit parameters, using ELITE to calculate the P-B constraint, and a “BCP” technique to calculate the KBM constraint [1]. EPED has been successfully compared to observed pedestal height for 270 cases on 5 tokamaks, finding agreement within ~20% [1–6]. Here we briefly discuss the EPED model, recent experimental tests, application to ELM-suppressed regimes, ITER predictions, and ongoing model development.

The present version of the EPED model proceeds from the conjecture that, while many mechanisms drive transport across the edge transport barrier region (ETB) in high performance H-mode discharges, the mechanisms which are strong enough to ultimately limit the pressure gradient, and total pressure, in the presence of strong sources and very strong $E \times B$ shear typical of the ETB, are the KBM and P-B. The P-B and KBM constraints are calculated using ELITE [7,8] and the BCP technique [1] on series of model equilibria, as shown in Fig. 1(a), yielding predictions of pedestal height and width (black circle).

As part of a 2011 US research milestone, EPED was extensively tested in a set of dedicated experiments on Alcator C-Mod and DIII-D, in which the magnetic field, current,

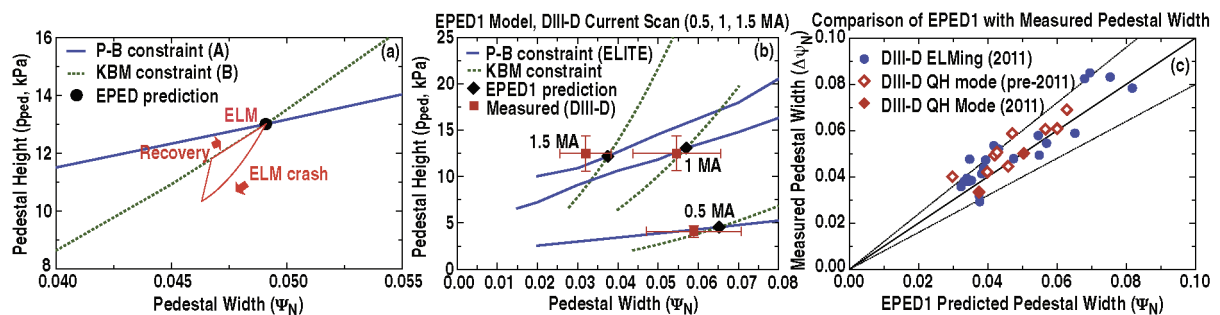


Fig. 1. (a) EPED predicts the pedestal height and width (black circle) as the intersection of calculated peeling-balloonning (solid line) and KBM (dotted line) constraints. A typical ELM cycle in this space is illustrated in red. (b) EPED predicted height and width (black diamonds) is compared to observations (red squares) for a current scan across 3 discharges on DIII-D. (c) Comparison of EPED predicted and observed pedestal width for a set of DIII-D discharges with accurate width measurements from a new Thomson system (blue circles) as well as from a set of 11 QH mode discharges (diamonds).

* See the Appendix of F. Romanelli et al., Proceedings of the 23rd IAEA Fusion Energy Conference 2010, Daejeon, Korea.

density and shape were varied, yielding large variation in pedestal height and width. On DIII-D, a new higher resolution Thomson system allowed very high accuracy measurements of both height and width. Figure 1(b) shows an example of a detailed test of the model using this new system. In this series of 3 discharges, the plasma current (I_p) was varied by a factor of 3 (0.5, 1.0, 1.5 MA), with the magnetic field (B_T) and plasma shape fixed. The calculated peeling-balloonning constraint [solid line, Fig. 1(b)] increases roughly linearly with current, with its increase slowing at lower q (higher current). The calculated KBM constraint (dotted line) increases more strongly with current, roughly as I_p^2 . As a result of the interaction of the KBM and P-B constraints, the EPED predicted pedestal height rises strongly ($\sim 3x$) with I_p as it is increased from 0.5 to 1.0 MA. However, the predicted height saturates and the width decreases dramatically as I_p is increased from 1.0 to 1.5 MA. The model predictions for both height and width are in reasonable agreement with the observations (red squares) for all three values of the current, successfully predicting the complex observed changes in height and width (changes which would not be described by a simple scaling law, or by P-B physics alone). In a broader statistical comparison, EPED predictions of the pedestal width were compared to a set of 24 cases from 14 shots with widths measured by the new DIII-D Thomson system. As shown in Fig. 1(c) (blue circles), agreement between the predicted and observed width is good, with a ratio of 0.94 ± 0.13 , and a correlation coefficient $r=0.91$ between predicted and observed width [and similar agreement in predicted height, as shown by blue circles in Fig. 2(a)]. An extensive set of experiments was conducted in ELMing H-mode discharges on Alcator C-Mod, varying the magnetic field (3.4, 5.3, 8 T) and the plasma current and density, and measuring pedestal structure with high resolution Thomson scattering [6]. Comparisons of measured pedestal structure to EPED find similar agreement as on DIII-D, as shown in Fig. 2(a) (green crosses). These comparisons extend tests of the model up to pressures within $\sim 3x$ of predicted ITER pressure (black diamond Fig. 2(a)], and to B_T and density equal to and exceeding ITER values. A similarity experiment was conducted on DIII-D, matching the C-Mod shape and dimensionless parameters, and found similar agreement with the model [blue + symbols in Fig. 2(a)].

Combining these recent tests of the EPED model with results from an extensive comparison to JET [5], as well as additional comparisons to AUG, DIII-D, and JT-60U [1–5], yields a dataset of 270 cases on 5 tokamaks, shown in Fig. 2(b). For this set of cases, the ratio of predicted to observed pedestal height is 0.98 ± 0.20 , with a correlation coefficient $r=0.92$.

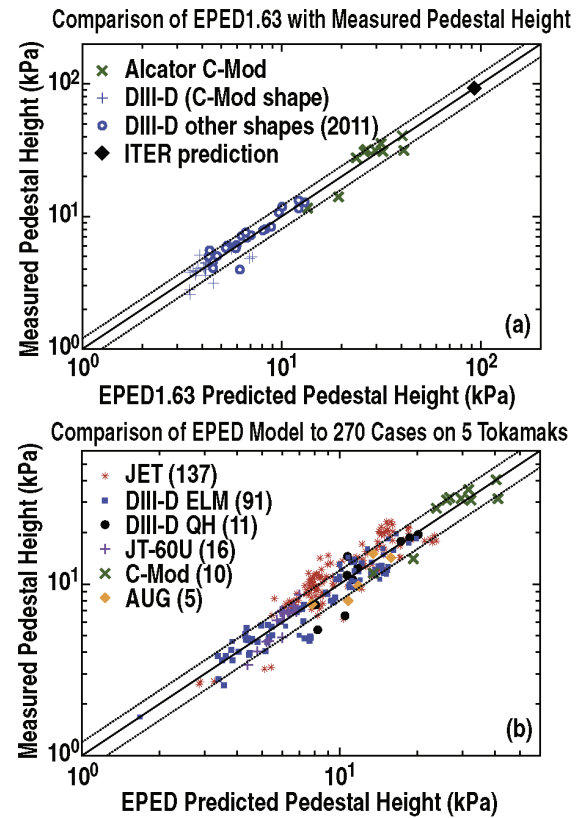


Fig. 2. (a) Comparison of EPED predicted pedestal height to observations on Alcator C-Mod and DIII-D, including a similarity experiment on C-Mod and DIII-D. An EPED prediction for the ITER baseline is also shown. (b) Comparison of predicted and observed pedestal height for a set of 270 cases on five tokamaks.

Statistically, this is consistent with $\sim 10\%-15\%$ measurement error and EPED accuracy to within $\sim 15\%-20\%$. Observed trends in pedestal height with I_p , B_T , plasma shape and density are generally well captured by the model.

The EPED model has been extensively used to predict the pedestal height and width in various scenarios on ITER, with more than 100 cases considered (e.g. [1,3]). Because ITER performance is expected to depend strongly on pedestal height, optimization in various scenarios is expected to be very important. An example study of predicted ITER pedestal pressure vs density at 2 different I_p values is shown in Fig. 3(a). Notably, the pedestal height is predicted to increase with pedestal density up to quite high values, exceeding the Greenwald density limit. Understanding this limit, as well as ensuring sufficient fuelling capability to reach high density may be important for ITER optimization.

One interesting aspect of the EPED model is that it predicts the existence of a regime in which very high pedestal pressure is possible, known as “Super H-Mode”. An example is shown in Fig. 3(b). For any value of the pedestal density, the standard EPED prediction (white lines) has a single value. However, for strongly shaped discharges, a second, or “Super H-Mode” region is potentially accessible via a dynamic optimization of the density (starting at moderate density and then raising the density to high values after the pedestal is fully developed). The EPED model predicts this regime should be accessible in high triangularity DIII-D, JET and ITER discharges, and there are preliminary indications of possible partial access on DIII-D and JET. For example, it has been observed in high triangularity JET discharges that when strong gas puffing is used to increase the pedestal density, high pedestal pressures, somewhat in excess of the standard EPED predictions, can be achieved [6,9], which may indicate at least partial access to the Super H-Mode regime. Further study of possible Super H-Mode access is planned.

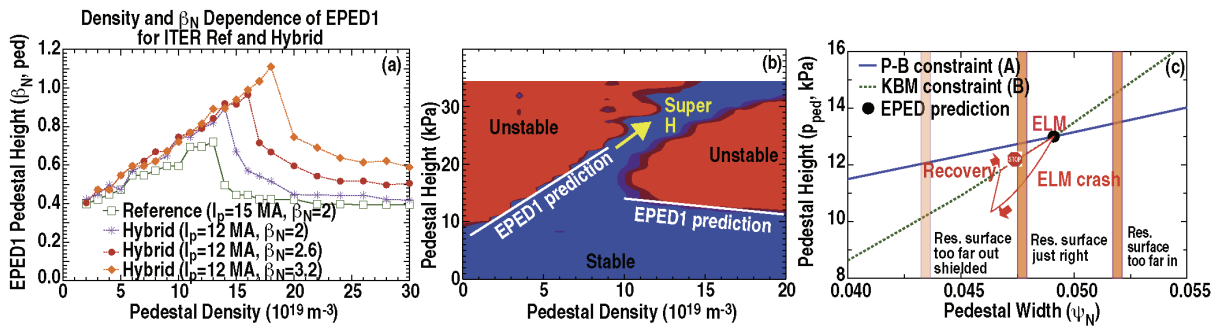


Fig. 3. (a) EPED predictions for ITER pedestal height as a function of pedestal density for ITER baseline (15 MA) and hybrid (12 MA) cases. (b) EPED predictions for pedestal height (white lines) are shown as a function of pedestal density for a high triangularity DIII-D case. Note in particular that a “Super H-Mode” region at very high pedestal pressure is potentially accessible by starting at lower density and then dynamically increasing the density in time to move up and to the right in this parameter space. (c) A working model for RMP ELM suppression is illustrated, showing that a region of increased transport (here associated with a rational surface, e.g. an island or stochastic region) can suppress the ELM if this region is in the proper location to constrain the broadening of the pedestal.

In addition to understanding the physics of pedestal structure in ELMing discharges, it is important to understand the physics of ELM-suppressed regimes, such as Quiescent H-mode (QH) [10], and ELM suppression by resonant magnetic perturbations (RMP) [11]. The EPED model has recently been applied to QH-mode discharges, finding similar agreement in predicted pedestal width and height as in ELMing discharges [red diamonds in Fig. 1(c), and black asterisks in Fig. 2(b)] [2]. This is consistent with earlier studies finding that the edge

harmonic oscillation (EHO) in QH mode is driven near the kink-peeling part of the P-B stability boundary [8], and with local gradients constrained by KBM. To understand RMP ELM-suppression it appears necessary to consider the dynamic ELM cycle, illustrated for example by the red lines and arrows in Figs 1(a) and 3(c). The ELM (or EHO in QH mode) is predicted to occur near the black circle, and the ELM can be prevented if the recovery part of the cycle is stopped, such that the pedestal does not continue to broaden and/or grow. We hypothesize that in RMP ELM suppression, broadening of the pedestal can be prevented by penetration of the RMP near the pedestal top. This requires a precise location of the RMP penetration, and offers an explanation for observed q -windows for ELM suppression and narrowing of the pedestal during ELM suppression [2]. Much additional work is needed to fully quantify this RMP working model.

The success of the EPED model has generated further interest in direct electromagnetic gyrokinetic (EMGK) studies of the pedestal region. EPED uses a simplified ballooning critical pedestal (BCP) technique to calculate the KBM constraint [1], which has been compared in several cases with direct EMGK calculations with codes such as GYRO [12], GS2 [13] and GEM [14]. In the “first stable” regime for the KBM, these comparisons are relatively straightforward, and the BCP technique reproduces EMGK calculations with reasonable accuracy. However, with strong shaping, low collisionality and/or high- q , plasmas can achieve a significant degree of second stability access to the KBM. While the BCP technique in EPED attempts to account for this, purely local EMGK calculations likely cannot be used to determine the KBM threshold in this limit. It is expected, based on MHD theory and simulation, that finite- n (non-local) effects are important. Initial work is ongoing with both local and non-local EMGK calculation to quantify the KBM in both first and 2nd stable regimes, as well as to study other relevant microinstabilities in the pedestal region.

In summary, the EPED model has been developed and extensively tested, finding ~20% agreement with observed pedestal height and width. The model has been successfully tested on ELMing and QH-mode discharges, and used in the development of a working model for RMP ELM suppression. Further model development and testing are ongoing including EMGK calculations and consideration of direct incorporation of such calculations in the model.

This work was supported by the US Department of Energy under DE-FG02-95ER54309, DE-AC05-00OR22725, DE-FG02-92ER54141, and by EURATOM and carried out within the framework of the European Fusion Development Agreement. The views and opinions expressed herein do not necessarily reflect those of the European Commission.

- [1] P.B. Snyder, *et al.*, Nucl. Fusion **51**, 103016 (2011).
- [2] P.B. Snyder, *et al.*, Phys. Plasmas **19**, 056115 (2012).
- [3] P.B. Snyder *et al.*, Phys. Plasmas **16**, 056118 (2009); Nucl. Fusion **49**, 085035 (2009).
- [4] R.J. Groebner *et al.*, Nucl. Fusion **50**, 064002 (2010); Nucl. Fusion **49**, 085037 (2009).
- [5] M. Beurskens, *et al.*, Phys. Plasmas **18**, 056120 (2011); H-Mode workshop (2011).
- [6] J.R. Walk *et al.*, Nucl. Fusion **52**, 063011 (2012).
- [7] H.R. Wilson *et al.*, Phys. Plasmas **9**, 1277 (2002).
- [8] P.B. Snyder *et al.*, Phys. Plasmas **9**, 2037 (2002); Nucl. Fusion **47**, 961 (2007).
- [9] M.J. Leyland *et al.*, “Pedestal width study in dense high triangularity ELMMy H-mode plasmas on JET,” in preparation (2012).
- [10] K.H. Burrell *et al.*, Plasma Phys. Control. Fusion **44**, A253 (2002); Plasma Phys. Control. Fusion **47**, B37 (2005).
- [11] T.E. Evans *et al.*, Phys. Rev. Lett **92**, 235003 (2004); Nature Phys. **2**, 419 (2006).
- [12] E. Wang, *et al.*, “Linear gyrokinetic analysis of a DIII-D H-Mode pedestal near ideal ballooning threshold,” submitted to Nucl. Fusion (2012).
- [13] D. Dickinson, *et al.*, Plasma Phys. Control. Fusion **53**, 115010 (2011).
- [14] W. Wan, *et al.*, “Global gyrokinetic simulation of tokamak edge pedestal instabilities,” submitted to Phys. Rev. Lett. (2012).